Combinatorial Mutagenesis and Structural Simulations in the Environment of the Redox-Active Tyrosine Y_Z of Photosystem II[†]

Hadar Kless and Wim Vermaas*

Department of Botany and Center for the Study of Early Events in Photosynthesis, Arizona State University, Tempe, Arizona 85287-1601

Received September 5, 1996; Revised Manuscript Received October 14, 1996[⊗]

ABSTRACT: Tyr161 of the D1 protein (Y_Z) is a redox component closely associated with the water-oxidizing complex of photosystem II. Y_Z reduces the primary donor $P680^+$, and Y_Z^{ox} is then rereduced by the manganese cluster that oxidizes water. We aimed to investigate whether water oxidation by $P680^+$ could occur through an alternative pathway in the absence of Tyr161. For this purpose, combinatorial mutagenesis was performed in residues presumed to be in the environment of Tyr161. Full sequence degeneracy was introduced in two regions of the D1 protein: at codons 157, 158, 160, 162, 163, 164, and 165, which are close to Y_Z by sequence, and at codons 186−191 which are assumed to be close to Y_Z in the tertiary structure; at position 161, the nucleotide combinations were designed to not give rise to a Tyr codon. The combinatorial DNA mixture was used to transform an obligate photoheterotrophic mutant (Y161W) of the cyanobacterium *Synechocystis* sp. PCC 6803, in which Trp at position 161 impairs photosynthetic activity. Transformants were selected in which photoautotrophic growth was restored, resulting in 11 viable mutants. In all of these mutants, however, a Tyr codon was found at position 161, introduced either by complex repair processes or as a result of PCR-induced mutations. Additional mutations found in residues neighboring Tyr161 mostly retained photosystem II properties similar to those of wild type. However, in two of these mutants, F**VE**YPI and FL**V**Y**N**I, photoautotrophic growth was impaired and the relative variable fluorescence was reduced. Computer simulations of the environment of Y_Z suggest that the position of Tyr161 varies with respect to some neighboring residues without major functional consequences. We conclude that Tyr161 fulfills a critical role through its chemical nature and positioning and that this function cannot be substituted by another residue at a nearby position.

Photosystem II (PSII)[1] is a part of the photosynthetic apparatus in cyanobacteria and in chloroplasts that utilizes light energy to catalyze plastoquinone reduction by water. The water oxidation complex (WOC) performs a unique activity found only in PSII. The WOC is located at the lumenal side of thylakoid membranes in close association with protein domains of the D1 protein—one of the two reaction center components of PSII. The WOC includes a tetramanganese cluster and Ca^{2+} and Cl^- ions that are closely associated with the redox-active tyrosine residue of the D1 protein (Tyr161, Y_Z) [for review, see Bricker and Ghanotakis (1996) and Diner and Babcock (1996)].

The chemistry of water oxidation in PSII is not clear. Recently, functional analogies between the WOC of PSII and other oxygen-dependent radical-containing metalloenzymes have been evaluated (Hoganson et al., 1995; Tommos et al., 1995). These enzymes, such as ribonucleotide reductase, have O_2/H_2O activating metal centers that abstract a H atom from the substrate through a radical (Pedersen & Finazzi-Agro, 1993; Sigel & Sigel, 1994). The reverse reaction, H abstraction from water by Y_Z^{ox}, may occur in the WOC. Upon absorption of a photon by the primary donor P680, an excited singlet state is formed, which can reduce a nearby pheophytin (Pheo) forming a $P680^+/Pheo^-$ state. Charge separation is stabilized when $Pheo^-$ is oxidized by Q_A and $P680^+$ is reduced by Y_Z. Y_Z^{ox} is then reduced by the WOC with reducing equivalents coming ultimately from water [for review, see Babcock (1995) and Britt (1996)].

The environment of Y_Z in the D1 protein has an analogous region in the reaction center protein D2. This region in D2 contains a redox-active tyrosine Y_D (D2-Tyr160), which does not seem to be a part of normal electron transfer at the donor side. Y_D is situated in a more hydrophobic environment as compared to that of Y_Z (Svensson et al., 1990; Ruffle et al., 1992). Y_D has clear hydrogen bond interaction with a nearby His residue (Tommos et al., 1993; Vermaas et al., 1993; Tang et al., 1993), and Y_Z seems to have a more dispersed hydrogen-bonding interaction (Tang et al., 1996). Mutations generated in the D1 protein that replace Tyr161 by Phe (Debus et al., 1988), Cys, Met, or His [see Diner and Babcock (1996)] impair photoautotrophic growth, and oxidized forms of these residues were not detected. Therefore, Y_Z seems to be an essential component at the donor side of PSII. We aimed to test this hypothesis.

In previous studies, combinatorial mutagenesis (Kless & Vermaas, 1995a) and spontaneous rearrangements (Kless & Vermaas, 1995b) were used to generate functional sequence combinations in highly conserved regions of the D1 protein. We aimed to apply these approaches to test whether alternative pathways for electron transfer around Y_Z might be generated in the immediate environment of this redox-

[†] This work was supported by Research Grant GM-51556 from the National Institutes of Health.

* Corresponding author. Tel: (602)-965-3698. Fax: (602)-965-6899. E-mail: wim@asu.edu.

[⊗] Abstract published in *Advance ACS Abstracts,* November 15, 1996.

[1] Abbreviations: D1 and D2, the two reaction center proteins of PSII; μE, μmol of photons; EPR, electron paramagnetic resonance; Q_A, the primary quinone of PSII; Q_B, the secondary quinone of PSII; P680, the primary donor of PSII; PCR, polymerase chain reaction; Pheo, pheophytin; PSII, photosystem II; Y_D, Tyr160 of the D2 protein; Y_Z, Tyr161 of the D1 protein.

S0006-2960(96)02240-4 CCC: $12.00

active residue. We found that Tyr161 could not be functionally replaced by the residues selected. Functional analysis coupled to computer simulations of mutations generated near D1-Tyr161 were used to assess structure−function relationships in the immediate environment of Y_Z.

MATERIALS AND METHODS

Strains and Growth Conditions. The Y161W[2] mutant of *Synechocystis* sp. PCC 6803 was obtained from R. Debus. This mutant, which contains mutations in two bases of the D1-Tyr161 codon, TAC to TGG, is an obligate photoheterotroph and did not yield any spontaneous pseudorevertants in our hands. Y161W contains the *psb*AII gene while the other two copies of *psb*A (*psb*AI and *psb*AIII) have been deleted (Debus et al., 1990). The wild-type strain used for comparative analysis (Kless et al., 1994) and growth conditions on plates and in liquid cultures (Kless & Vermaas, 1995a) have been described.

Mutant Preparation. We have prepared combinatorial mutations in the *psb*AII gene coding for the D1 protein through a procedure of overlapping PCR (Figure 1). The DNA sequences of oligonucleotides used for mutagenesis are indicated in Table 1. The linear DNA fragments (AM_2B and BM_1A) amplified by PCR were used to transform the Y161W mutant followed by selection for restoration of photoautotrophy on BG-11 plates (Kless & Vermaas, 1995a). Single colonies were isolated, and genomic DNA was extracted from each strain. The *psb*AII gene was amplified from the genomic DNA of the selected photoautotrophic transformants by PCR using oligonucleotides A and B. The amplified DNA fragments were separated on TBE−agarose gel (0.8% w/v), and the agarose piece containing the DNA band was cut out from the gel and frozen at −20 °C. The agarose piece was then thawed at 37 °C, and the DNA was isolated by spinning through an Ultrafree-MC 0.45 μm filter unit (Millipore). The DNA was precipitated overnight at −20 °C in the presence of (final concentrations) 5% (w/v) PEG 8000, 1.3 mM $MgCl_2$, 100 mM sodium acetate (pH 5.2), and 50% (v/v) 2-propanol and then washed twice with 100% ethanol. The DNA was resuspended in water, and about 250 ng of DNA along with 1 pmol of the appropriate primer were used for automated sequencing using an ABI 377 DNA sequencer (Perkin Elmer).

Analysis of Photosynthetic Performance. Determination of photoautotrophic growth rates (Kless & Vermaas, 1995b) and quantitation of PSII on a chlorophyll basis by [^{14}C]diuron binding (Vermaas et al., 1990a) have been described. Oxygen evolution rates were measured at saturating light conditions and in the presence of 0.1 mM 2,5-dimethyl-*p*-benzoquinone (DMBQ) and 0.5 mM $K_3Fe(CN)_6$ (Kless & Vermaas, 1995a).

Chlorophyll fluorescence measurements were used to determine the relative amount of variable fluorescence (F_v/F_m) (Kless & Vermaas, 1995a), charge recombination rates between Q_A^- and the donor side, and Q_A^- accumulation induced by consecutive flashes. A pulse-modulated fluorometer (Walz) with the fluorescence software FIP (Q_A-Data) was used for these measurements. Cells for fluorescence measurements were suspended in 25 mM Hepes−NaOH (pH 7.2) and placed (0.3 mL at 20 μg of chlorophyll/mL) in a 12 mm piece cut from the bottom of a 15 mL plastic tube (Falcon). This was attached directly to the light guide and was wrapped with aluminum foil in order to increase the fluorescence signal. Prior to all fluorescence measurements, 0.1 mM DMBQ and 0.5 mM $K_3Fe(CN)_6$ were added to the cell suspension in order to oxidize the quinone pool.

Charge recombination between Q_A^- and the donor side was followed from flash-induced fluorescence decay in the presence of diuron. Cells were incubated in darkness in the holder for 2 min in the presence of 80 μM diuron (final methanol concentration <0.2%). The measuring light (0.15 μE m^{-2} s^{-1}) was turned on right before the flash in order to prevent accumulation of Q_A^- due to this light. The half-time of charge recombination ($t_{1/2}$) was determined by fitting the fluorescence decay curve [normalized as $(F - F_o)/F_o$] with one exponential decay component and an offset: $a_1e^{-kt} + F_{of}$, where a_1 is the amplitude of the decay, k is the decay rate constant, and F_{of} is a residual component. These variables were given initial values that were adjusted through a nonlinear least-squares fitting (Kless & Vermaas, 1995a). From k the $t_{1/2}$ of the decay was calculated.

Accumulation of Q_A^- was induced by consecutive flashes followed by actinic light. Cells were incubated in darkness for 1 min in the presence of 10 mM hydroxylamine, then 50 μM diuron was added, and cells were incubated for an additional 2 min in darkness. Variable fluorescence was induced by 10 consecutive flashes given at 800 ms intervals followed by a 10 s period of continuous actinic light (115 μE m^{-2} s^{-1}).

Protein Simulation. Structural simulation of the Y_Z region of the D1 protein was performed using Look 2.0 software on a Silicon Graphics workstation. The simulations were performed using the SegMod application in the Look 2.0 program (Molecular Applications Group), which applies homology modeling through fragment-matching and energy minimization algorithms (Levitt, 1992). Atomic coordinates of the L and M subunits of the *Rhodopseudomonas viridis* reaction center (Deisenhofer et al., 1985) were taken from the 1PRC file from the Brookhaven Protein Data Bank. The protein alignments between D1 and the L subunit and between D2 and M were as in Michel and Deisenhofer (1988).

RESULTS

Mutant Preparation. *Synechocystis* sp. PCC 6803 can be transformed with linear DNA that integrates into the genome by homologous recombination and leads to targeted gene replacement. Degenerate combinations of codons were introduced into the *psb*AII gene of the Y161W mutant by PCR-mediated mutagenesis (Figure 1). Two degenerate regions were designed using three M_1 (I−III) and one M_2 oligonucleotides (Table 1). At one of the first two nucleotides of the 161 codon, the M_1 oligonucleotides contain a combination of only three different bases so that the Tyr codons TAC and TAT cannot be formed at this position (see Table 1). Fully degenerate codons were designed at positions 160 and 162 in oligonucleotides M_1-I and M_1-II and at positions 157, 158, 162, 164, and 165 in oligonucleotide M_1-III. The M_2 oligonucleotide was synthesized with fully degenerate codons at positions 186−191. In this sequence, His190 and Phe186 are assumed to be close to Y_Z in the

[2] The nomenclature of the mutants prepared in this study corresponds to amino acids in positions 158−163 of the D1 protein, where residues that were modified as compared to wild type are in boldface; amino acids in mutant nomenclature are indicated by their one-letter code and in single positions by the three-letter code; numbering of amino acids in D1 and D2 refers to those of *Synechocystis* sp. PCC 6803.

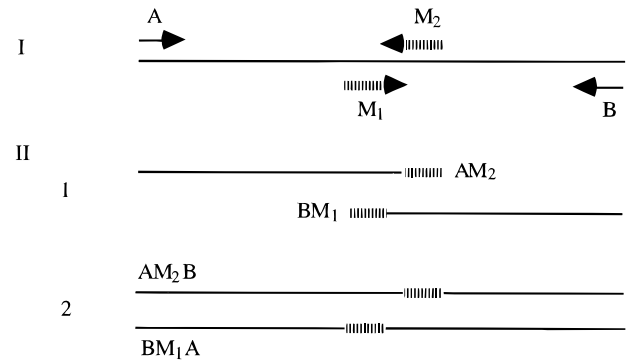

FIGURE 1: Two-step PCR mutagenesis procedure to introduce degenerate sequences at two separate locations. (I) Primers A, B, M_1, and M_2 were designed to match certain sequences in the *psb*AII gene coding for the D1 protein (Table 1). Several codons, 157, 158, 160, 162, 164, and 165, were synthesized in primer M_1 to contain degenerate combination of nucleotides, while at position 161 the primers were designed to not give rise to Tyr codons. In primer M_2, the codons 186−191 near His190 were degenerate (see Materials and Methods). (II) 1. The *psb*AII gene of the Y161W mutant was amplified by PCR using primer combinations AM_2 and BM_1. 2. The corresponding PCR fragments were purified from agarose gel and mixed for a second PCR using primers A and B, which result in two different fragments (AM_2B and BM_1A; 1383 bp each) carrying degenerate nucleotides. A mixture of these two DNA fragments was used to transform the Y161W strain followed by selection for photoautotrophic competence. Degenerate combinations of nucleotides are designated as (|||||).

tertiary structure in analogy with the environment of Y_D in the D2 protein (Svensson et al., 1990). Three separate PCR reactions, each with a different M_1 oligonucleotide, were performed in order to construct the DNA fragments AM_2B and BM_1A (Figure 1). These fragments were used to transform the Y161W mutant cells in 10 separate experiments. After transformation, the cells were grown on BG-11 plates that support only photoautotrophic growth. Eleven colonies with restored photoautotrophic capability were isolated after about 2−3 weeks. Single colonies were then isolated to ensure homogeneity in the *psb*AII allele. In order to verify that mutation(s) restoring photoautotrophy are located only in the mutated region, DNA fragments from the mutants were amplified by PCR using the oligonucleotides A and B and then were used to transform the Y161W mutant followed by selection for photoautotrophy.

DNA containing the *psb*AII gene from the photoautotrophic strains was amplified by PCR using primers A and B, and the nucleotide sequence of both strands was determined near the degenerate locations. The nucleotide sequence and the corresponding translation of the 11 photoautotrophic strains are presented in Table 2. Although not included in the oligonucleotides used for mutagenesis, Tyr codons were found at position 161 in all of the photoautotrophic strains. Five of these codons are TAC as in wild type while the other six are TAT; the almost equal distribution of these codons may suggest random events that induce these unintentional changes. The 161 codons in the M_1 oligonucleotides contained either XNN (where N = A, C, G, and T and X = A, C, and G) or NZN (Z = C, G, and T). In these codon combinations, a single change is sufficient to regenerate a Tyr codon. This may have occurred during PCR mutagenesis or after transformation—during recombination or upon another repair event. In all mutants analyzed, the DNA sequence in positions 186−191 of D1 that was degenerate in oligonucleotide M_2 remained as in wild type, indicating that all 11 mutants were generated through integration of BM_1A (Figure 1).

Most of the other positions degenerated by the mutagenesis procedure contained changes in the DNA that also translated to changes in the protein sequence (Table 2). Mutations have occurred often at position 162, which was degenerate in all of the three M_1 oligonucleotides, and at position 160, which was degenerate in M_1-I and M_1-II. Positions 157, 158, 164, and 165 were modified in M_1-III, of which only positions 158 and 164 were found to be mutated in one of the photoautotrophic strains, while codons 157 and 165 remained unaffected. Surprisingly, two other positions, 159 and 163, contained mutations in some of the mutants although they were not degenerate in any of the oligonucleotides used for mutagenesis.

Functional Characterization of the Mutants. The mutant strains were analyzed in terms of their photoautotrophic growth rates, oxygen evolution rates, the relative variable fluorescence, and charge recombination rates (Table 3). As expected, the Y161W mutant does not grow photoautotrophically, has no oxygen evolution, and does not show significant variable fluorescence.

Photoautotrophic growth rates of wild type and of most of the mutant strains were found to be quite similar; only in the mutants F**VE**YPI and FL**VYN**I was the growth rate about 2.5-fold slower. Differences in photoautotrophic growth rates may reflect altered electron transfer kinetics or PSII amounts.

Oxygen evolution was monitored under saturating light conditions and in the presence of electron acceptors. This measurement may identify impairments that become rate limiting for linear electron transfer and water oxidation in PSII. Mutants that had reduced rates of oxygen evolution (by about 20−40%) contained a nonconservative mutation at position 160 or Glu or Asn at position 162.

The relative variable fluorescence, F_v/F_m, may relate to the amount of centers capable of reducing Q_A and has been used for indirect quantitation of PSII centers (Chu et al., 1994). The F_v/F_m ratio measured in the presence of diuron was diminished particularly in the F**VE**YPI and FL**VYN**I mutants as compared to that of wild type (Table 3). Addition of hydroxylamine, an electron donor to oxidized P680, did not enhance the F_v/F_m ratio in these mutants (data not shown). However, these data should not be interpreted as a decrease in the number of PSII centers: according to the diuron binding assay, which measures the amount of PSII centers more directly through binding of specific inhibitors, the amount of centers in these mutants is comparable to that of wild type (Figure 2).

The charge recombination assay monitors the variable fluorescence yield corresponding to the Q_A^- concentration. Q_A^- was induced by a single flash, and the forward electron transfer from Q_A^- was blocked by 80 μM diuron. The rate of Q_A^- disappearance (reflecting an oxidation) via a back-reaction with the donor side was monitored by the fluorescence yield decay (Figure 3). Charge recombination rates may be affected as a result of changes in the steady-state concentration of $P680^+$ or in the relative positioning of any of the components. Whereas the amplitudes of charge recombination in the mutants F**VE**YPI and FL**VYN**I were about four times smaller than that of wild type (Figure 3), the half-times of the single phase decay component ($t_{1/2}$) were comparable (Table 3).

The accumulation of Q_A^- in the presence of diuron and hydroxylamine was induced by consecutive flashes. Diuron

Table 1: Oligonucleotides Used for Overlapping PCR Mutagenesis

oligonucleotide	DNA sequences[a]
A	CCAAAAGGCCCTCTGTTTACC
B	GGCAATCAAGATCAGCAATCAG
M_1-I[b]	GCCACCGCCGTATTCTTGNNN**XNN**NNNATTGGTCAAGGCTCCTTCTC
M_1-II[b]	GCCACCGCCGTATTCTTGNNN**NZN**NNNATTGGTCAAGGCTCCTTCTC
M_1-III[b]	CCGCTGCCACCGCCNNNNNNTTGATC**XNN**NNNATTNNNNNNGGCTCCTTCTCTGATGG
M_2	GGAAGGGGTGCATCAGGATNNNNNNNNNNNNNNNNNNNCACGATCATGAAGTTGAAGG

[a] DNA sequences of oligonucleotides are presented from 5′ to 3′. Primers A and B correspond to nucleotides −193/−173 and 1189/1168, respectively, of the *psb*AII gene of *Synechocystis* 6803. The 5′ end of oligonucleotides M_1-I and -II is at position 460, that of M_1-III is at position 455, and that of M_2 is at position 592. [b] N, equal amounts of all four bases; X, an equal mixture of A, C, and G; Z, an equal mixture of C, G, and T. Nucleotides at codon 161 of the M_1 oligonucleotides (bold type) were designed to not give rise to Tyr codons—TAC and TAT.

Table 2: DNA and Protein Sequences of Wild Type and Mutant Strains

strain	DNA and protein sequences[a]								
	157				161				165
wild type	GTA	TTC	TTG	ATC	TAC	CCC	ATT	GGT	CAA
	V	F	L	I	Y	P	I	G	Q
Y161W					TGG				
					W				
FLIY**E**I						GAA			
						E			
FL**V**YPI				GTG					
				V					
FL**VYG**I				GTG	TAT	GGT			
				V	Y	**G**			
FL**VYN**I				GTG		AAT		GGG	
				V		**N**		G	
FLIY**SS**				ATA	TAT	TCA	AGT		
				I	Y	**S**	**S**		
GLLYPI		GGC		CTA	TAT	CCG			
		G		**L**	Y	P			
FL**TYCM**				ACG		TGC	ATG		
				T		**C**	**M**		
F**VTYPM**			GTG	ACA		CCA	ATG		
			V	**T**		P	**M**		
FL**TYT**I				ACG	TAT	ACT			
				T	Y	**T**			
FL**TYV**I				ACA	TAT	GTG			
				T	Y	**V**			
F**VE**YPI			GTG	GAA	TAT	CCA			
			V	**E**	Y	P			

[a] Nucleotide sequences of the *psb*AII gene and the corresponding amino acid sequences (157−165) of the D1 protein are shown for wild type, the Y161W mutant, and the photoautotrophic strains that were generated by combinatorial mutagenesis of Y161W (the nomenclature refers to the protein sequence at positions 158−163; modified residues are in bold type). In the mutant sequences, only the codons that were modified as compared to those of wild type are indicated; amino acids that were altered are indicated in bold type. DNA sequences are presented from 5′ to 3′. Note that two positions in the mutants, 159 and 163, were not degenerate in the oligonucleotides used for mutagenesis. In all mutants, positions 186−191 of D1 that were degenerate in oligonucleotide M_2 were identical to those in wild type.

Table 3: Functional Characteristics of Wild Type and Mutant Strains

strain[a]	doubling time[b] (hrs)	oxygen evolution[c] (% of WT)	F_v/F_m[d]	recombination[e] $t_{1/2}$ (s)	recombination[e] relative amplitude	F_1/F_v[f]
wild type	16	100	0.45	0.20	0.64	0.58
Y161W	0	0	na	na	na	na
FLIY**E**I	22	70	0.39	0.24	0.66	0.51
FL**V**YPI	17	100	0.46	0.23	0.63	0.61
FL**VYG**I	17	100	0.33	0.26	0.59	0.75
FL**VYN**I	39	70	0.20	0.20	0.52	0.56
FLIY**SS**	16	100	0.35	0.22	0.62	0.73
GLLYPI	18	100	0.27	0.24	0.60	0.48
FL**TYCM**	22	60	0.34	0.19	0.60	0.63
F**VTYPM**	20	80	0.40	0.21	0.63	0.62
FL**TYT**I	23	60	0.38	0.24	0.61	0.70
FL**TYV**I	19	80	0.42	0.19	0.58	0.62
F**VE**YPI	41	70	0.18	0.22	0.53	0.43

[a] For mutant nomenclature see Table 1; the wild-type sequence is FLIYPI. [b] Photoautotrophic doubling times; the rates are an average of three to four measurements that vary by about 20%. [c] Oxygen evolution rates measured under saturating light conditions are shown as a percentage of the wild-type rates (220 ± 50 μmol·(mg of Chl)$^{-1}$·h^{-1}); the values are an average of three measurements. [d] The relative variable fluorescence (F_v/F_m) in the presence of diuron was measured using intact cells of a similar chlorophyll content (66 μg of Chl/mL) and volume (0.3 mL); variability in this measurement is about 15% as calculated from three to four measurements. [e] The half-times ($t_{1/2}$) of charge recombination between Q_A^- and the manganese cluster were calculated from fluorescence decay curves (Figure 3). The relative amplitude reflects the fraction that decays within 1 s and was calculated from the fitting equation (a_1; see Materials and Methods). [f] F_1/F_v determines the amplitude of the fluorescence after the first flash relative to the total variable fluorescence measured in the presence of diuron and hydroxylamine (Figure 4). na: not available.

blocks forward electron transfer from Q_A^-, and hydroxyl amine disturbs the manganese cluster and donates electrons directly to Y_Z^{ox} or $P680^+$. In this assay, each flash leading to charge separation gives rise to Q_A^- that does not recombine with the donor side since P680 is reduced, directly or indirectly, by hydroxylamine. This assay monitors changes in the efficiency of $P680^+$ reduction by the manganese complex or through hydroxylamine. In all of the mutants, the accumulation of Q_A^- was comparable to that of wild type. In the mutants F**VE**YPI and FL**VYN**I, the variable fluorescence amplitude was about 25% (Figure 4), but the amplitude of the first flash (F_1/F_v) in these mutants was comparable to that of wild type and the other mutants (Table 3). In both wild type and mutants in the presence of diuron the variable fluorescence yield was decreased slightly upon addition of hydroxylamine; the reason for this decrease is unclear.

Protein Modeling. In the absence of a detailed structure of PSII, a possible conformation of the D1 protein in the mutated area was computed through homology modeling. Homology modeling adopts the coordinates of the homologous protein and then matches small fragments of the protein to be modeled with those from structures of known proteins in the data bank; the best fitted fragments are averaged and then refined by energy minimization (Levitt, 1992). To determine the possibly most favorable structure of the D1 protein, we utilized sequence homology with the L subunit of the reaction center of the photosynthetic bacterium *Rps.*

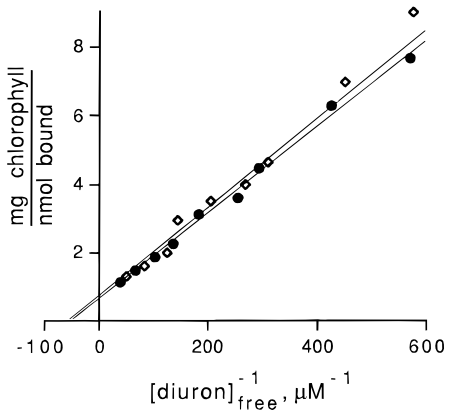

FIGURE 2: Quantitation of PSII centers on a chlorophyll basis by [^{14}C]diuron binding in intact cells of wild type (circles) and the mutant F**VE**YPI (diamonds). The cells were incubated in the presence of variable concentrations of [^{14}C]diuron and in the presence or absence of saturating concentrations of atrazine; both are competitive inhibitors that bind in the Q_B niche. The amount of bound diuron was determined from the concentration that could be displaced by atrazine. The double-reciprocal plot presents the inverses of the amount of free [^{14}C]diuron and bound diuron/mg of chlorophyll. The *Y*-intersection corresponds to the number of chlorophylls per PSII center, and the *X*-intersection reflects the inverse of the diuron dissociation constant *in vivo*.

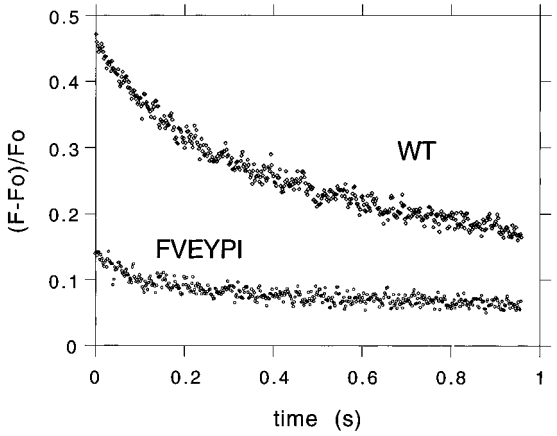

FIGURE 3: Decay kinetics of flash-induced variable fluorescence in the presence of diuron. Intact cells of wild type and F**VE**YPI were incubated in the dark for 2 min in the presence of 80 μM diuron. The fluorescence then was followed after a single flash representing roughly the concentration of Q_A^- in PSII. The fluorescence yield decays after the flash due to charge recombination between Q_A^- and the manganese cluster mediated through Pheo, P680, and Y_Z.

viridis for which the crystal structure is known (Deisenhofer et al., 1985). The extent of sequence homology and the precise alignment are crucial for prediction by the homology modeling approach. Although donor-side activities differ between PSII and the bacterial reaction center, the region of helices *C* and *D* seems to be reasonably similar in terms of length and conservation of key residues (Michel & Deisenhofer, 1988).

Homology modeling was conducted for wild type and seven of the mutants. The models of wild type and FL**V**Y**N**I in the Y_Z region are shown in Figure 5. According to this model, in wild type D1 the residue closest to the phenoxy group of Tyr161 is Gln165 (3.3 Å). The distances between the phenoxy group of Tyr161 and residues Asp170 (4.8 Å), Phe186 (4.2 Å), and His190 (6.8 Å) are somewhat larger in this model. These distances differ somewhat from models that have been developed using different premises and software; for example, in the model of Svensson and Styring

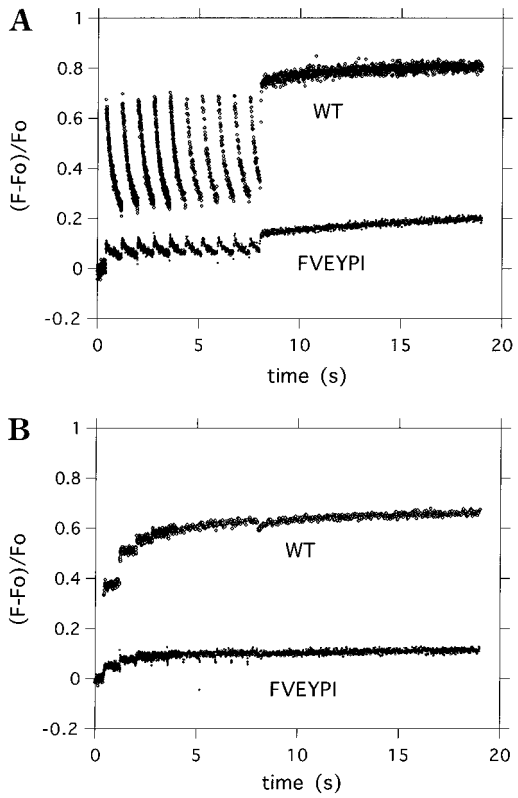

FIGURE 4: Accumulation of Q_A^- by consecutive flashes. Cells of the wild type and the mutant F**VE**YPI were incubated in darkness in the presence of diuron (A) or hydroxylamine and diuron (B), and variable fluorescence was induced by 10 consecutive flashes (given at 800 ms intervals) followed by continuous actinic light. The curve shape of the mutant FL**V**Y**N**I (not shown) is very similar to that of F**VE**YPI.

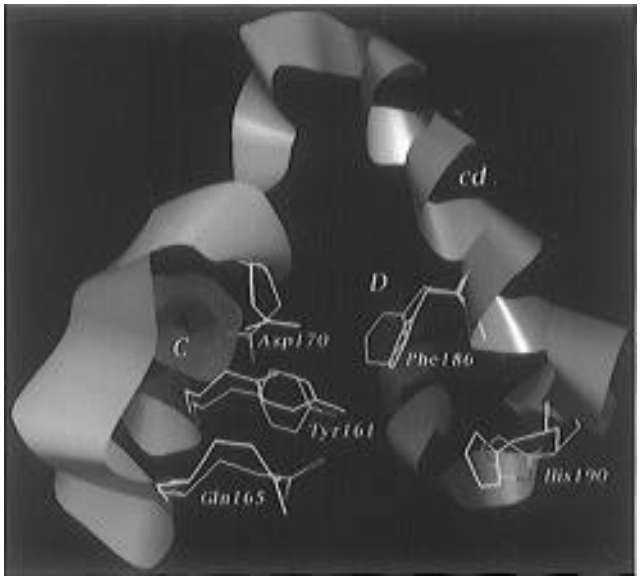

FIGURE 5: Structural simulations of the Y_Z region of the D1 protein constructed by homology modeling based on the structure of the L subunit of the bacterial reaction center of *Rps. viridis*. The protein domain in the simulated structure is viewed from underneath the membrane plane; the transmembrane helices *C* and *D* and the parallel helix *cd* are indicated. The protein backbone of wild type is shown in ribbon style, and the residues of wild type (gray) and the mutant FL**V**Y**N**I (yellow) that may be involved in water oxidation are indicated. Colors in wild type represent oxygen (red) and nitrogen (blue) atoms.

(1995) the Tyr161−His190 distance is 4 Å. However, differences in the predicted distances because of methodical and software reasons are of little consequence for our

Table 4: Residue Distances in Structural Simulations[a]

strain[b]	Tyr161 Gln165	Tyr161 Asp170	Tyr161 Phe186	Tyr161 His190	Gln165 Asp170
wild type	3.3 (3.9)	4.8	4.2	6.1 (4.8)	5.1
FLIY**E**I	6.8 (5.3)	6.8	3.4	6.3 (3.2)	5.9
FLV**Y**G**I**	7.1 (3.4)	6.5	3.7	6.0 (3.7)	6.1
FLV**Y**N**I**	7.0 (3.9)	6.0	3.8	5.3 (3.9)	5.4
FLIY**SS**	7.3 (3.4)	5.2	3.7	6.7 (4.2)	5.7
FL**T**Y**CM**	6.7 (3.3)	6.2	3.7	5.9 (3.3)	5.3
F**V**T**Y**P**M**	6.8 (4.2)	5.2	4.0	7.0 (3.4)	5.7
F**V**E**Y**PI	5.2 (3.8)	5.5	3.7	5.6 (5.2)	5.2
Variance	1.9 (0.42)	0.50	0.056	0.31 (0.54)	0.13

[a] Distances between side-chain groups of D1 and D2 residues were determined from structural simulations of the wild type and some of the mutants. Distances were measured between D1 residues Tyr161 (phenoxy), Gln165 (amine), Asp170 (the closest oxygen in the carboxylate), His190 (the closest ring nitrogen), and Phe186 (C_4 of the phenol ring); the distance between Gln165 and Asp170 was measured between the carbons of the amide and carboxylate groups of the side chains, respectively. Distances between residues of D2 (in parentheses) include Tyr160, Gln164, and His189 and were calculated as for D1 residues. Structures of D2 of wild type and putative mutants were constructed by computer simulations based on the M subunit of *Rps. viridis* as homologue. Distances are given in Å. For mutant nomenclature see Table 1; the wild-type sequence is FLIYPI.

arguments as our focus is on comparison of the structures between wild type and mutants modeled using the same software and assumptions. It should be kept in mind that the results presented here and in any PSII modeling study do not take into account many of the complexities of PSII such as the presence of neighboring proteins. In the simulated structures of wild type and the seven mutants, the positions of residues Tyr161, Gln165, Asp170, Phe186, and His190 were compared in terms of the distance between some of these residues (Table 4). Some of the calculated distances between two residues remained relatively constant in wild type and the mutants, indicating that the residues did not move much with respect to each other as a function of the mutations. However, the calculated distance between positions 161 and 165 was found to be increased by about a factor of 2 in all mutants.

As a control, the structure of the environment of Y_D in the D2 protein was similarly simulated using the coordinates of the M subunit of *Rps. viridis* (not shown). The distances between D2 residues Tyr160, Gln164, and His189, which are analogous to D1 residues Tyr161, Gln165, and His190, respectively, were compared (Table 4). For D2, the large effect of mutations on the distance between residues 160 and 164 is not observed; the size of the effect is similar to that in the distance between D2 residues 160 and 189.

DISCUSSION

Combinatorial Mutagenesis To Study the Environment of Y_Z. In this study we applied combinatorial mutagenesis to several residues of the Y_Z environment to investigate whether alternative electron transfer pathways can be engineered in the absence of Tyr161. The mutagenesis procedure introduced combinatorial mutations in two separate DNA fragments (Figure 1), which are expected to separately integrate into the cyanobacterial genome more often than to cointegrate into the same gene copy. The number of molecules (N) that contain certain sequence combinations in the degenerate codons is estimated from $N = \ln(1 - P)/\ln(1 - f)$, where P is the probability to find a certain codon in a degenerate sequence of three nucleotides and f is the codon fraction in this sequence (the number of specific codons out of the 64 codon possibilities). The codon fraction ranges between 0.0156 (one codon) and 0.094 (six codons). To estimate the number of molecules containing any codon combination in a completely degenerate pool, we used a median value of $f = 0.047$ (three codons); the fraction of c independent codon positions is 0.047^c. N calculated for $P = 0.95$ is 62 for one codon increasing exponentially to 2.8×10^8 for six codons. However, the transformation efficiency in *Synechocystis* sp. PCC 6803, using a PCR-amplified DNA of 1.38 kbp (the size of the AB fragment), becomes a limiting factor (about $2 \times 10^3/\mu$g of DNA). About 40 μg of DNA (20 μg for each PCR fragment—AM_2B and BM_1A; see Figure 1) that was used in separate transformation experiments should have yielded about 4×10^4 potential transformation events in the Y_Z region (by the BM_1A fragment). Assuming that each event resulted from a single molecule, only combinations of three or less specific codons ($N = 2.9 \times 10^4$) could have sufficient probability ($P = 0.95$) to be represented in the degenerate DNA pool. We therefore expect that if a certain combination of three specific codons or less in the protein sequences can support a functional analog alternative to Tyr161 in either of the degenerate locations, the immediate sequence (residues 158−163) and the remote sequence (residues 186−191) of the D1 protein, it would have been identified in these experiments. However, such transformants are expected to occur less frequently if a combination of more than three codons in one or both regions is required or if some of the codon combinations are functionally deleterious.

The fortuitous events restoring Tyr at its original position appeared to occur at a frequency of 10^{-3}−10^{-4} as 11 colonies were isolated from about 10^4−10^5 transformants. A spontaneous reversion of this codon in the Y161W mutant was not observed (requires concomitant changes in two nucleotides). Tyr161 may have been restored as a result of mutations occurring during PCR mutagenesis (frequency of about 10^5 per one error) or through DNA repair mechanisms. The unplanned mutations in residues 159 and 163 of the D1 protein found in two of the mutants may also have occurred through these mechanisms.

Environment of Y_Z and Water Oxidation: Functional Analysis. Y_Z carries out two main functions: oxidation of the manganese cluster and reduction of $P680^+$. The positioning of Y_Z should be important for efficient and rapid reduction of $P680^+$, which otherwise could recombine with Q_A^-. In the combinatorial mutagenesis experiments Tyr161 was restored through DNA rearrangements, but not a single Y_Z alternative was generated by direct transformation. Therefore, in the context of the degeneracy applied in this study, no other residue appears to be able to take over the function of Tyr161 and to serve as electron transport intermediate between the WOC and P680.

The other viable mutations that were isolated can be used to evaluate the involvement of the immediate environment of the Y_Z region on redox reactions involving P680 and the WOC. Position 160 in the photoautotrophic strains contained the amino acids Val, Leu, Thr, or Glu, whereas position 162 had Glu, Gly, Asn, Ser, Cys, and Val, and position 163 harbored the residues Ser, Thr, and Met. All of these positions could thus accommodate different types of amino acids, but position 162 seems more permissible than 160. Interestingly, none of the mutants that were isolated was

drastically impaired in terms of Y_Z. All mutants displayed relatively normal charge recombination kinetics and significant oxygen evolution yields.

However, two of the isolated mutants, F**VE**YPI and FL**VYN**I, showed a small amplitude of the relative variable fluorescence F_v/F_m even in the presence of diuron and hydroxylamine. These mutations did not destabilize PSII measured as the amount of centers that retained normal inhibitor binding capacity at the Q_B niche. This may reflect heterogeneity of PSII centers in these mutants: some centers may have an inactive Y_Z possibly because of donor side damage. This would cause a lack of $P680^+$ reduction by donor side components and thus a lack of variable fluorescence in these centers ($P680^+$ is a quencher of variable fluorescence). If this indeed is the case, then hydroxylamine appears to be unable to reduce $P680^+$ directly in this system, as addition of hydroxylamine did not increase variable fluorescence (Figure 4).

However, in PSII centers giving rise to variable fluorescence the rate of electron transfer from Q_A^- to the donor side through charge recombination in the F**VE**YPI and FL**VYN**I mutants was comparable to that of wild type. Also, the ratio F_1/F_v measured by flash-induced fluorescence rise in the presence of diuron and hydroxylamine is relatively normal in these mutants. Therefore, among the apparently heterogeneous population of PSII centers, those that contain active centers appear to have normal thermodynamic properties of Y_Z.

Environment of Y_Z and Water Oxidation: Homology Modeling. Protein modeling may be able to simulate whether functional characteristics of the mutants are related to structural perturbations. We attempted to compare protein simulations and functional characteristics of the mutants to evaluate possible interactions in the region of Y_Z. Changes in the orientation of Tyr161 or in its immediate environment may (in)directly affect donor side stability and/or electron transfer efficiency. Analysis of the structural data suggests that mutations neighboring Y_Z may drastically affect the positioning of this residue with respect to Gln165. This suggests that a rearrangement of these residues does not impair Y_Z function.

Electron paramagnetic characteristics of Y_Z suggest that Tyr161 is hydrogen bonded with another atom. Unlike the clear hydrogen bond characterized for between Tyr160 and probably His189 in the D2 protein, the hydrogen bond involving Y_Z is more dispersed (Tang et al., 1996), which may correspond to a flexible Tyr161. We find variability in the distances between Tyr161 and Gln165 as a function of nearby mutations. According to our simulations, in wild type these residues are close to each other (3−4 Å) and within hydrogen-bonding distance. In light of the possible flexibility of Tyr161, we suggest that in certain conformations or redox states this residue could interact with Gln165, facilitating proton transfer following hydrogen abstraction from water. However, in view of the minor effects of the mutations on Y_Z function and the increased distances between Tyr161 and Gln165 in structural simulations of these mutants, other residues in this region may also participate in proton transfer from Y_Z.

Although these protein models should be treated as not more than relatively rough approximations of the actual structure, combining functional analysis and structural simulations of many mutants may provide valuable information for constructing structural and functional models of proteins including the WOC.

ACKNOWLEDGMENT

We thank Dr. R. Debus for the Y161W strain of *Synechocystis* sp. PCC 6803, Dr. S. Bingham for nucleotide synthesis and automated sequencing, and the Molecular Applications Group for guidance in using the Look software.

REFERENCES

Babcock, G. T. (1995) in *Photosynthesis: From Light to Biosphere* (Mathis, P., Ed.) Vol. II, pp 229−234, Kluwer Academic Publishers, Dordrecht.

Bricker, T. M., & Ghanotakis, D. F. (1996) in *Oxygenic Photosynthesis: The Light Reactions* (Ort, D. R., & Yocum, C. F., Eds.) pp 113−136, Kluwer Academic Publishers, Dordrecht.

Britt, R. D. (1996) in *Oxygenic Photosynthesis: The Light Reactions* (Ort, D. R., & Yocum, C. F., Eds.) pp 137−164, Kluwer Academic Publishers, Dordrecht.

Chu, H.-A., Nguyen, P., & Debus, R. J. (1994) *Biochemistry 33*, 6137−6149.

Debus, R. J., Barry, B. A., Sithole, I., Babcock, G. T., & McIntosh, L. (1988) *Biochemistry 27*, 9071−9074.

Debus, R. J., Nguyen, P., & Conway, A. B. (1990) in *Current Research in Photosynthesis* (Baltscheffsky, M., Ed.) Vol. I, pp 829−832, Kluwer Academic Publishers, Dordrecht.

Deisenhofer, J., Epp, O., Miki, K., Huber, R., & Michel, H. (1985) *Nature 318*, 618−624.

Diner, B. A., & Babcock, G. T. (1996) in *Oxygenic Photosynthesis: The Light Reactions* (Ort, D. R., & Yocum, C. F., Eds.) pp 213−247, Kluwer Academic Publishers, Dordrecht.

Hoganson, C. W., Lydakis-Simantiris, N., Tang, X.-S., Tommos, C., Warncke, K., Babcock, G. T., Diner, B. A., McCracken, J., & Styring, S. (1995) *Photosynth. Res. 46*, 177−184.

Kless, H., & Vermaas, W. F. J. (1995a) *J. Mol. Biol. 246*, 120−131.

Kless, H., & Vermaas, W. F. J. (1995b) *J. Biol. Chem. 270*, 16536−16541.

Kless, H., Oren-Shamir, M., Malkin, S., McIntosh, L., & Edelman, M. (1994) *Biochemistry 33*, 10501−10507.

Levitt, M. (1992) *J. Mol. Biol. 226*, 507−533.

Michel, H., & Deisenhofer, J. (1988) *Biochemistry 27*, 1−7.

Pedersen, J. Z., & Finazzi-Agro, A. (1993) *FEBS Lett. 325*, 53−58.

Ruffle, S. V., Donnelly, D., Blundell, T. L., & Nugent, J. H. A. (1992) *Photosynth. Res. 34*, 287−300.

Sigel, H., & Sigel, A., Eds. (1994) *Metal Ions in Biological Systems, Metalloenzymes involving amino acid residues and related radicals*, Vol. 30, Marcel Dekker, New York.

Svensson, B., & Styring, S. (1995) in *Photosynthesis: From Light to Biosphere* (Mathis, P., Ed.) Vol. I, pp 647−650, Kluwer Academic Publishers, Dordrecht.

Svensson, B., Vass, I., Cedergren, E., & Styring, S. (1990) *EMBO J. 9*, 2051−2059.

Tang, X.-S., Chisholm, D. A., Dismukes, G. C., Brudvig, G. W., & Diner, B. A. (1993) *Biochemistry 32*, 13742−13748.

Tang, X.-S., Zheng, M., Chisholm, D. A., Dismukes, G. C., & Diner, B. A. (1996) *Biochemistry 35*, 1475−1484.

Tommos, C., Davidsson, L., Svensson, B., Madsen, C., Vermaas, W. F. J., & Styring, S. (1993) *Biochemistry 32*, 5436−5441.

Tommos, C., Tang, X.-S., Warncke, K., Hoganson, C. W., Styring, S., McCracken, J., Diner, B. A., & Babcock, G. T. (1995) *J. Am. Chem. Soc. 117*, 10325−10335.

Vermaas, W. F. J., Charité, J., & Shen, G. (1990) *Z. Naturforsch. 45c*, 359−365.

Vermaas, W. F. J., Styring, S., Schröder, W. P., & Andersen, B. (1993) *Photosynth. Res. 38*, 249−263.

BI962240Q